ACS BIO & MED CHEM Au
AN OPEN ACCESS JOURNAL OF THE AMERICAN CHEMICAL SOCIETY

pubs.acs.org/biomedchemau
Article

Biosynthetic Pathways of Alaremycin and Its Derivative: Inhibitors of Porphobilinogen Synthase in Porphyrin Biosynthesis from *Streptomyces* sp. A012304

Mio Okui,[‡] Yuki Noto,[‡] Jun Kawaguchi, Noritaka Iwai, and Masaaki Wachi*

Cite This: *ACS Bio Med Chem Au* 2025, 5, 310–319
Read Online

ACCESS | Metrics & More | Article Recommendations | Supporting Information

ABSTRACT: The antibiotic alaremycin (5-acetamido-4-oxo-5-hexenoic acid, **1**), isolated from *Streptomyces* sp. A012304, structurally resembles 5-aminolevulinic acid (ALA), a precursor in porphyrin biosynthesis, and inhibits porphobilinogen synthase, the enzyme responsible for catalyzing the first common step of this pathway. In our previous study, the biosynthetic gene cluster responsible for alaremycin production—composed of *almA* (ALA synthase homologue), *almB* (*N*-acetyltransferase), *almC* (oxidoreductase), and *almE* (MFS-type transporter)—was identified, and a potential biosynthetic pathway was proposed. In this study, the biosynthetic pathway of **1** was confirmed by detecting intermediates using the liquid chromatography−mass spectrometry/MS (LC-MS/MS) analysis of extracts from *Escherichia coli* cells transformed with the biosynthetic genes, followed by *in vitro* reconstitution of the biosynthetic reactions using purified enzymes. AlmA catalyzed the condensation of L-serine and succinyl-CoA to produce 5-amino-6-hydroxy-4-oxohexanoic acid (**2**), AlmB catalyzed the *N*-acetylation of **2** to produce 5-acetamido-6-hydroxy-4-oxohexanoic acid (**3**), and AlmC catalyzed the dehydration of **3** to form **1**. The AlmC-catalyzed reaction may involve a two-step mechanism including reduction by NADH and oxidation by Fe^{3+}. Additionally, a novel derivative of **1** was identified in the culture broth of the producer strain, and its structure was determined as 5,6-dihydroalaremycin (5-acetamido-4-oxohexanoic acid, **4**). It was revealed that **4** is synthesized via the same biosynthetic pathway but with AlmA and AlmB utilizing L-alanine as the amino acid precursor instead of L-serine.

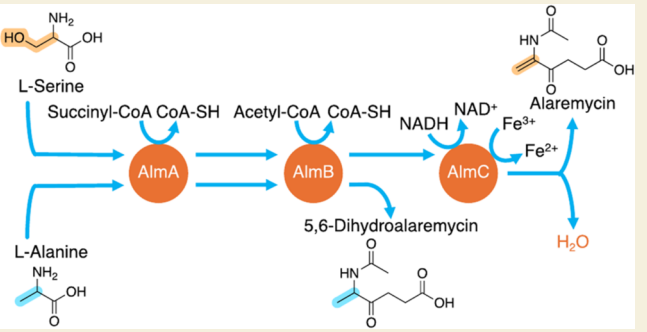

KEYWORDS: *alaremycin, 5-aminolevulinic acid, antibiotics, biosynthesis, porphobilinogen synthase, porphyrin, Streptomyces*

INTRODUCTION

Since the discovery of penicillin by Fleming in 1928, numerous antibiotics have been isolated from microorganisms.[1,2] These antibiotics, along with their chemically modified derivatives, have been widely used to treat bacterial infections and save countless lives. Over the past century, the human lifespan has increased by 23 years in large part due to the effectiveness of these treatments.[3] However, the recent emergence of drug-resistant pathogens poses a serious threat to human health. In particular, the increase of multidrug-resistant pathogens, including multidrug-resistant *Pseudomonas aeruginosa* (MDRP),[4−6] vancomycin-resistant *Staphylococcus aureus* (VRSA),[7−9] vancomycin-resistant *Enterococcus* (VRE),[10,11] and multidrug-resistant tuberculosis (MDR-TB),[12−14] has become an alarming issue. It is estimated that by 2050, drug-resistant bacterial infections could cause up to 10 million deaths annually.[15] To combat this growing threat, the discovery and development of new antibiotics are urgently needed.

One approach to addressing the growing issue of drug resistance is the discovery of novel drugs that target previously unexplored mechanisms. In a previous study, we performed random screening using culture broths of actinomycetes isolated from soil samples and tested them using the blue assay method.[16] This assay is designed to detect the formation of chromosome-less cells (anucleate cells) due to the inhibition of chromosome segregation. Through this screening, we identified a new antibiotic, named alaremycin (**1**), in the culture broth of *Streptomyces* sp. A012304.[17] The structure of compound **1** closely resembles 5-aminolevulinic acid (ALA), a key precursor in porphyrin biosynthesis. Subsequent studies revealed that alaremycin inhibits porphobilinogen synthase (PBGS), the enzyme that catalyzes the first common step in porphyrin biosynthesis, by competing with its substrate, ALA.

Received: February 10, 2025
Revised: February 28, 2025
Accepted: March 3, 2025
Published: March 7, 2025

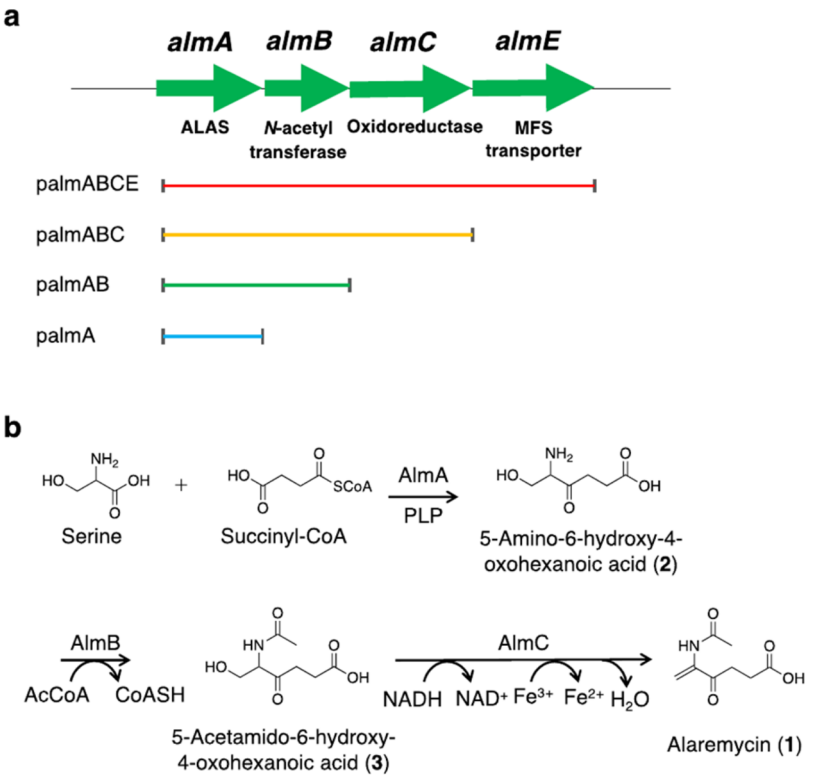

Figure 1. Biosynthetic gene cluster of alaremycin and its proposed biosynthetic pathway. (a) Alaremycin biosynthetic gene cluster in *Streptomyces* sp. A012304. The DNA fragments cloned into plasmids for identifying biosynthetic intermediates are shown. *almA* (ALAS homologue), *almB* (*N*-acetyltransferase), *almC* (oxidoreductase), and *almE* (MFS-type transporter). (b) Proposed biosynthetic pathway of alaremycin. AlmA catalyzes the condensation of L-serine and succinyl-CoA to produce compound 2. AlmB acetylates compound 2 using acetyl-CoA to produce compound 3. AlmC dehydrates compound 3 to produce alaremycin (compound 1).

Crystallographic analysis of alaremycin-bound PBGS from *P. aeruginosa*, a human pathogen, showed that a single alaremycin molecule occupies two distinct ALA binding sites, lysine-205 and lysine-260.[18] Based on this three-dimensional (3D) structure, chemical synthesis of alaremycin derivatives was conducted to enhance antibiotic activity, and some of these derivatives exhibited improved inhibitory activity against PBGS *in vitro*.[19]

In addition, our previous studies successfully identified the biosynthetic gene cluster responsible for alaremycin production, consisting of the *almA*, *almB*, *almC*, and *almE* genes (Figure 1a), and we proposed a potential biosynthetic pathway for **1** (Figure 1b).[20] The *almA* gene encodes a homologue of 5-aminolevulinic acid synthase (ALAS), an enzyme that catalyzes the condensation of glycine and succinyl-CoA to produce ALA. Given the structural differences between alaremycin and ALA, it was hypothesized that AlmA catalyzes the condensation of L-serine and succinyl-CoA to generate the first intermediate, 5-amino-6-hydroxy-4-oxohexanoic acid (**2**). The *almB* gene encodes an *N*-acetyltransferase, which was predicted to catalyze the *N*-acetylation of **2** to form the second intermediate, 5-acetamido-6-hydroxy-4-oxohexanoic acid (**3**). The *almC* gene encodes an oxidoreductase, suspected to catalyze the dehydration of **3**, ultimately producing **1**. Finally, the *almE* gene encodes an MFS-type transporter, which was proposed to export **1** out of the cell.

In a previous study, AlmA was shown to catalyze the condensation of L-serine and succinyl-CoA using a spectrophotometric assay coupled with α-ketoglutarate dehydrogenase, although the reaction product (compound **2**) was not detected.[20] The enzymatic activities of AlmB and AlmC were not explored in that study.

Notably, one of the biosynthetic enzymes, AlmA, which catalyzes the first step of alaremycin biosynthesis, shares structural and enzymological similarities with 5-aminolevulinic acid synthase (ALAS). While ALAS catalyzes the condensation of glycine and succinyl-CoA, AlmA catalyzes a similar reaction using L-serine and succinyl-CoA. Given these similarities, an ancestral sequence reconstruction study was performed, suggesting that AlmA-like antibiotic-synthesizing enzymes may have been evolutionary ancestors of ALAS.[20]

In this study, we elucidated the complete biosynthetic pathway of alaremycin (**1**) through the liquid chromatography−mass spectrometry/MS (LC-MS/MS) analysis and *in vitro* reconstruction of the biosynthetic enzyme reactions. Furthermore, we identified a novel derivative of **1** in the culture broth of the alaremycin-producing strain *Streptomyces* sp. A012304. The insights gained from this work not only enhance our understanding of the biosynthesis of this class of antibiotics but also provide valuable information for discussing the evolutionary origins of ALAS. Additionally, this knowledge could be leveraged for the fermentation of novel alaremycin derivatives through biotechnological modifications of the biosynthetic genes.

RESULTS

Identification of Biosynthetic Intermediates Using *E. coli* Cells Transformed with the Biosynthetic Genes

To verify the proposed biosynthetic pathway, we first aimed to identify the intermediate molecules using *Escherichia coli* cells

https://doi.org/10.1021/acsbiomedchemau.5c00045
ACS Bio Med Chem Au 2025, 5, 310−319

transformed with the biosynthetic genes. The culture supernatants of transformed *E. coli* cells were extracted with ethyl acetate at pH 2, and the extracts were subjected to LC-MS analysis. As shown in Figure 2a, an ion peak with a retention

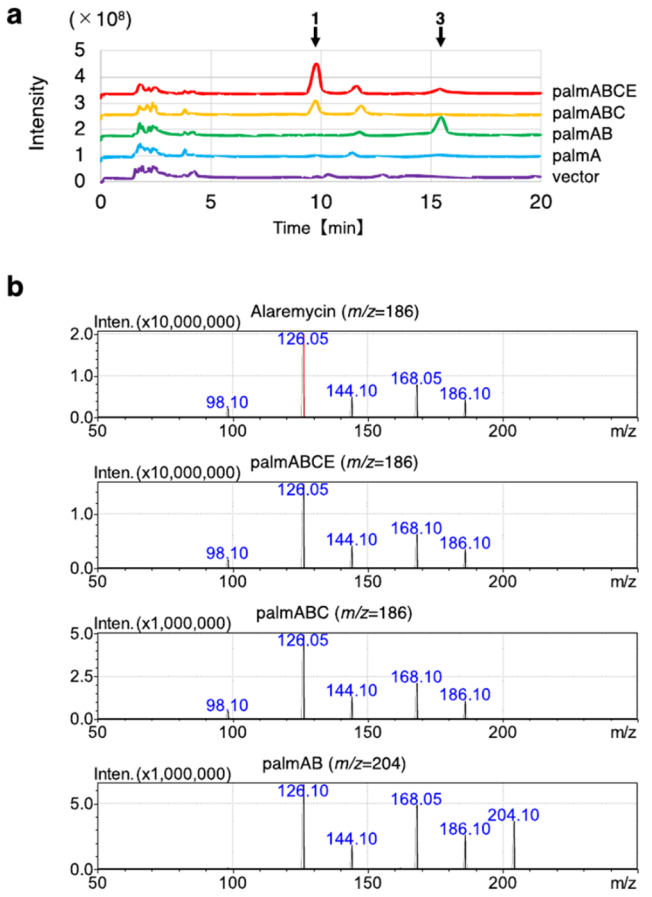

Figure 2. LC-MS/MS analysis of the culture supernatants from *E. coli* cells transformed with plasmids carrying alaremycin biosynthetic genes. (a) Total ion chromatograms of ethyl acetate extract fractions are shown. From top to bottom: *E. coli* transformed with palmABCE, palmABC, palmAB, palmA, and the vector control. Ion peaks corresponding to compounds 1 and 3 are indicated by arrows at the top of the chromatogram. (b) MS/MS fragment patterns of ion species with the indicated m/z values, as shown in Supporting Figure S1. From top to bottom: ion species with m/z = 186 derived from authentic alaremycin, ion species with m/z = 186 from the extract of *E. coli* transformed with palmABCE, ion species with m/z = 186 from the extract of *E. coli* transformed with palmABC, and ion species with m/z = 204 from the extract of *E. coli* transformed with palmAB.

time (RT) of 9.8 min was detected in the extract from *E. coli* cells transformed with the plasmid palmABCE, which carries the entire biosynthetic gene cluster. This peak was absent in the control *E. coli* cells transformed with the empty vector plasmid pTrc99A. In the MS spectrum of this peak, an ion species with m/z = 186 was observed, corresponding to the expected m/z value of the proton adduct $[M + H]^+$ of **1** (M_W = 185) (Supporting Figure S1a (authentic sample) and S1b). Additionally, an ion species with m/z = 208, corresponding to the expected m/z value of the sodium adduct $[M + Na]^+$ of **1**, was also detected (Supporting Figure S1a (authentic sample) and S1b). The ion species with m/z = 186 was further analyzed by MS/MS. As shown in Figure 2b, its fragmentation pattern was identical to that of authentic **1**. Based on these results, we confirmed that *E. coli* cells transformed with palmABCE successfully produced **1**. Similarly, *E. coli* cells transformed with palmABC also produced alaremycin, though in smaller amounts compared to *E. coli*/palmABCE (Figure 2 and Supporting Figure S1c). This reduced production is likely due to AlmE functioning as an exporter of **1**. There are several reports showing that exporters from *Streptomyces* species functioned in *E. coli* cells.[21,22]

E. coli cells transformed with palmAB or palmA did not produce **1**. However, another ion peak with an RT of 15.5 min was detected in the extract from *E. coli*/palmAB (Figure 2a). This peak was also present in smaller amounts in the extract from *E. coli*/palmABCE. In the MS spectrum of this peak, an ion species with m/z = 204 was detected, corresponding to the expected m/z value of the proton adduct $[M + H]^+$ of **3** (M_W = 203) (Supporting Figure S1d). Additionally, an ion species with m/z = 226, corresponding to the expected m/z value of the sodium adduct $[M + Na]^+$ of **3**, was observed (Supporting Figure S1d). MS/MS analysis revealed that the fragmentation pattern of the ion species with m/z = 204 closely resembled that of **1** (Figure 2b). The ion species with m/z = 204 fragmented into an ion with m/z = 186, corresponding to protonated **1**, and other fragment ions (m/z = 168, 144, and 126) that matched those of **1**. It is likely that the ion species with m/z = 204 underwent dehydration ($-H_2O$) to generate the ion species with m/z = 186 (Supporting Figure S2). Based on these results, we confirmed that *E. coli*/palmAB produced the second intermediate **3**.

In contrast, we were unable to detect an ion peak corresponding to the first intermediate **2** in the ethyl acetate extract of *E. coli* cells transformed with palmA (Figure 2a). We hypothesized that **2** was not efficiently partitioned into the ethyl acetate layer due to its higher hydrophilicity compared to that of **1** and **3**. To address this, we analyzed the supernatant fraction after acetone precipitation of the culture supernatant from *E. coli*/palmA by LC-MS. As expected, an ion peak with an RT of 14.7 min was detected in *E. coli*/palmA but was absent in the vector control (Figure 3a). In the MS spectrum, an ion species with m/z = 162 was observed, corresponding to the expected m/z value of the proton adduct $[M + H]^+$ of **2** (M_W = 161) (Supporting Figure S3). MS/MS analysis revealed that the fragmentation pattern of the ion species with m/z = 162 was similar to that of **1** (Figure 3b). The fragment ions (m/z = 144, 126, and 98) closely matched those of alaremycin. It appears that the ion species with m/z = 162 underwent dehydration ($-H_2O$) to generate an ion species with m/z = 144 (Supporting Figure S2). Based on these findings, we confirmed that *E. coli*/palmA produced the first intermediate **2**.

In Vitro Reconstitution of Biosynthetic Reactions Using Purified Enzymes

We then performed *in vitro* reconstitution of the biosynthetic reactions by using purified enzymes. His-tagged AlmA, AlmB, and AlmC proteins, with N-terminal tags, were expressed in *E. coli* BL21(DE3) and purified using Ni-affinity resin columns (Supporting Figure S4).

First, we investigated the initial reaction catalyzed by the AlmA protein. AlmA belongs to the α-oxoamine synthase family, which includes ALAS and requires pyridoxal 5′-phosphate (PLP) as a coenzyme for activity. When AlmA with PLP was incubated with L-serine and succinyl-CoA, LC-MS analysis detected an ion peak with a retention time (RT) of 15.8 min (Figure 4a). MS/MS analysis of the ion species

https://doi.org/10.1021/acsbiomedchemau.5c00045
ACS Bio Med Chem Au 2025, 5, 310−319

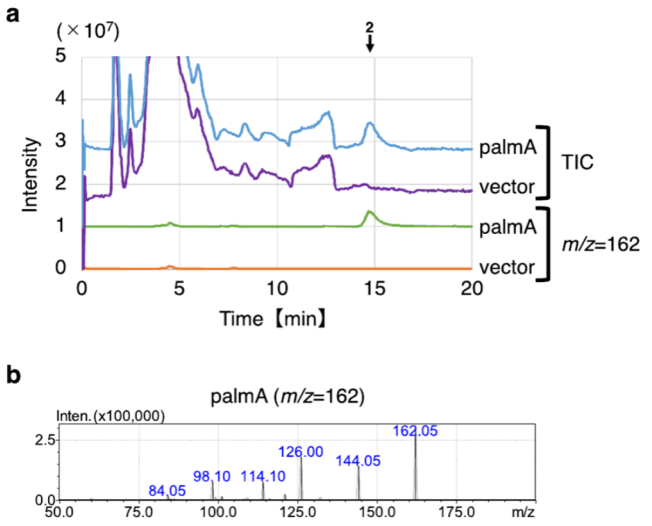

Figure 3. LC-MS/MS analysis of the culture supernatant from *E. coli* cells transformed with palmA. (a) Total ion chromatograms (TICs) and the extracted ion chromatograms (m/z = 162) of acetone-precipitated supernatant fractions are shown. The top chromatogram represents *E. coli* transformed with palmA, and the bottom chromatogram shows the vector control. The ion peak corresponding to compound 2 is indicated by an arrow at the top of the chromatogram. (b) MS/MS fragment pattern of the ion species with m/z = 162, derived from the extract of *E. coli* transformed with palmA, as shown in Supporting Figure S3.

with m/z = 162 confirmed it as the first intermediate **2** (Figure 3b and Supporting Figure S5). Even when the AlmA reaction was carried out without the addition of PLP, the reaction product was still produced. Therefore, we inferred that AlmA was copurified with PLP. From these results, we concluded that AlmA catalyzes the condensation of L-serine and succinyl-CoA in the presence of PLP to produce **2**, as suggested in our previous findings.[20]

Next, we investigated the second step of the reaction, catalyzed by AlmB. Since AlmB is annotated as an *N*-acetyltransferase, acetyl-CoA was added to the reaction mixture as an acetyl group donor. To generate **2** as the substrate for AlmB, AlmA with PLP, L-serine, and succinyl-CoA was also included in the reaction mixture. As shown in Figure 4b, LC-MS analysis detected an ion peak with an RT of 15.3 min.

MS/MS analysis of the ion species with m/z = 204 confirmed it as the second intermediate **3** (Figure 2b and Supporting Figure S5). These results indicate that AlmB catalyzes the acetylation of the amino group of **2** using acetyl-CoA as the acetyl group donor to produce **3**.

Next, we examined the third step of the reaction catalyzed by AlmC. AlmC is annotated as an oxidoreductase of the Gfo/Idh/MocA family.[23] A typical protein structure in this family consists of two main domains: an N-terminal dinucleotide-binding domain with a Rossmann fold and a C-terminal α/β domain involved in substrate binding and oligomerization.[23] As expected, AlmC contains an NAD-binding motif (GXGXXG) in its N-terminal domain;[24] therefore, NADH

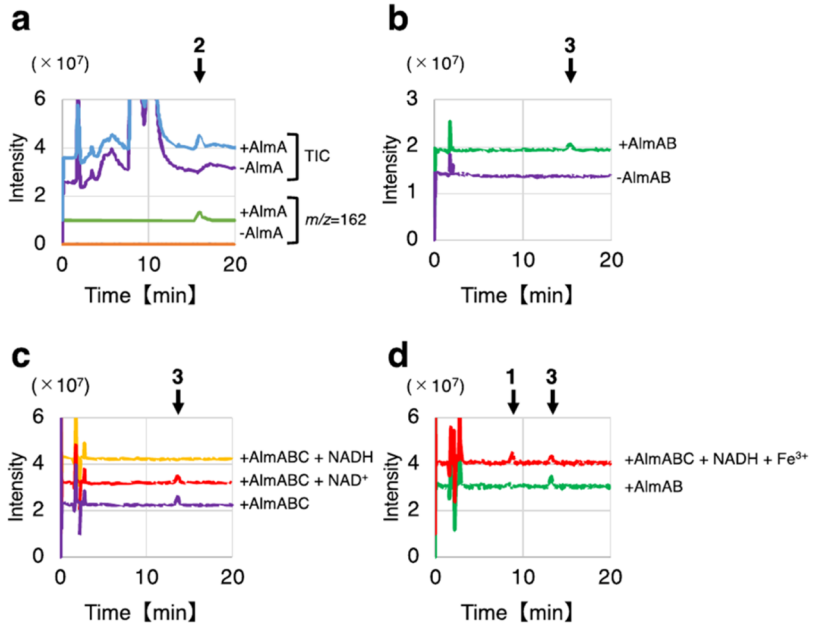

Figure 4. LC-MS analysis of the *in vitro* enzyme reaction mixtures. Total ion chromatograms of supernatant fractions from acetone precipitation (TIC) (a) or ethyl acetate extract fractions (b–d) are shown. Ion peaks corresponding to compounds 1–3 are indicated by arrows at the top of the chromatograms. (a) Enzymatic reactions were performed with 10 mM L-serine, 0.2 mM succinyl-CoA, and 20 μM PLP in the presence (+AlmA) or absence (−AlmA) of 2 μM AlmA. The extracted ion chromatograms (m/z = 162) are shown below the TIC. (b) Enzymatic reactions were performed with 10 mM L-serine, 0.2 mM succinyl-CoA, 20 μM PLP, and 0.2 mM acetyl-CoA in the presence (+AlmAB) or absence (−AlmAB) of 2 μM AlmA and 2 μM AlmB. (c) Enzymatic reactions were performed with 10 mM L-serine, 0.2 mM succinyl-CoA, 20 μM PLP, and 0.2 mM acetyl-CoA in the presence of 2 μM AlmA and 2 μM AlmB for 2 h. Subsequently, 2 μM AlmC was added to the reaction mixture either without (+AlmABC) or with 0.2 mM NADH (+AlmABC + NADH) or 0.2 mM NAD^+ (+AlmABC + NAD^+), which was incubated for an additional hour. (d) Enzymatic reactions were performed with 10 mM L-serine, 0.2 mM succinyl-CoA, 20 μM PLP, and 0.2 mM acetyl-CoA in the presence of 2 μM AlmA and 2 μM AlmB for 3 h (+AlmAB). Then, 2 μM AlmC, 0.2 mM NADH, and 3 mM $FeCl_3$ were added to the reaction mixture, which was further incubated for an additional 2 h (+AlmABC + NADH + Fe^{3+}).

https://doi.org/10.1021/acsbiomedchemau.5c00045
ACS Bio Med Chem Au 2025, 5, 310–319

or NAD^+ was included in the reaction mixture. First, the AlmA and AlmB reactions were carried out for 2 h to accumulate the second intermediate **3**. Then, AlmC was added to the reaction mixture either without or with NADH or NAD^+, and the mixture was incubated for an additional hour. As shown in Figure 4c, the amount of compound **3** produced by AlmA and AlmB decreased upon the addition of AlmC and NADH. The consumption of NADH was also suggested by a decrease in its specific absorption at 340 nm (Supporting Figure S6). However, unexpectedly, the anticipated product **1** was not detected. These results suggest that AlmC used **3** as a substrate with NADH acting as a reducing agent, leading to the formation of an unknown intermediate that was undetectable by this LC-MS analysis. It is possible that the unknown intermediate was not extracted into the ethyl acetate layer or was trapped within the enzyme's active site. Notably, neither AlmC alone nor the combination of AlmC and NAD^+ affected the amount of **3** (Figure 4c).

To complete the AlmC-catalyzed reaction to give **1** from the unknown intermediate produced by the reduction of **3**, we hypothesized that oxidation and dehydration of the unknown intermediate are required. To test this, we added Fe^{3+} ions to the AlmC reaction mixture as an electron acceptor. As anticipated, the formation of **1** was observed when $FeCl_3$ was included in the AlmC reaction with NADH (Figure 4d and Supporting Figure S5). However, the addition of $FeCl_3$ alone did not facilitate the reaction in the absence of NADH (Supporting Figure S7a). The addition of Fe^{2+} along with NADH also facilitated the reaction to produce **1** (Supporting Figure S7b). Since Fe^{2+} is readily oxidized to Fe^{3+} under atmospheric conditions but the opposite dose does not happen, we inferred that Fe^{3+} is required for the reaction. Other metal ions, such as Mg^{2+} and Ca^{2+}, showed no effect. From these results, we concluded that AlmC catalyzes the reduction of second intermediate **3**, in the presence of NADH, followed by an Fe^{3+}-dependent reaction that leads to the production of **1**.

Based on these findings, we conclude that alaremycin is synthesized by AlmA, AlmB, and AlmC using L-serine and succinyl-CoA as starting materials.

Identification of a New Alaremycin Derivative Produced by *Streptomyces* sp. A012304

During this study, we observed that the alaremycin-producing strain *Streptomyces* sp. A012304 generated an unknown compound that could not be detected by the high-performance liquid chromatography (HPLC) analysis monitoring the absorption at 256 nm (A_{256}). As shown in Figure 5a, only **1** was detected in the ethyl acetate extract of the culture supernatant from strain A012304 during the HPLC analysis. However, when the same extract was analyzed by LC-MS monitoring the total ion intensity, an additional ion peak with an RT of 10.9 min was observed alongside the ion peak for **1** (RT = 9.2 min) (Figure 5b). In the MS spectrum of this new ion peak (RT = 10.9 min), an ion species with m/z = 188 was detected, which is 2 units larger than the proton adduct of **1** (Supporting Figure S8). Additionally, an ion peak with m/z = 210 was detected, corresponding to a sodium adduct, also **2** units larger than that of **1** (Supporting Figure S8). These results suggest that the A012304 strain produces a compound with a molecular weight 2 units larger than that of **1**. Since this compound exhibited no absorption at 256 nm, we hypothesized that it is a hydrogen adduct of **1** at the C5−C6 position,

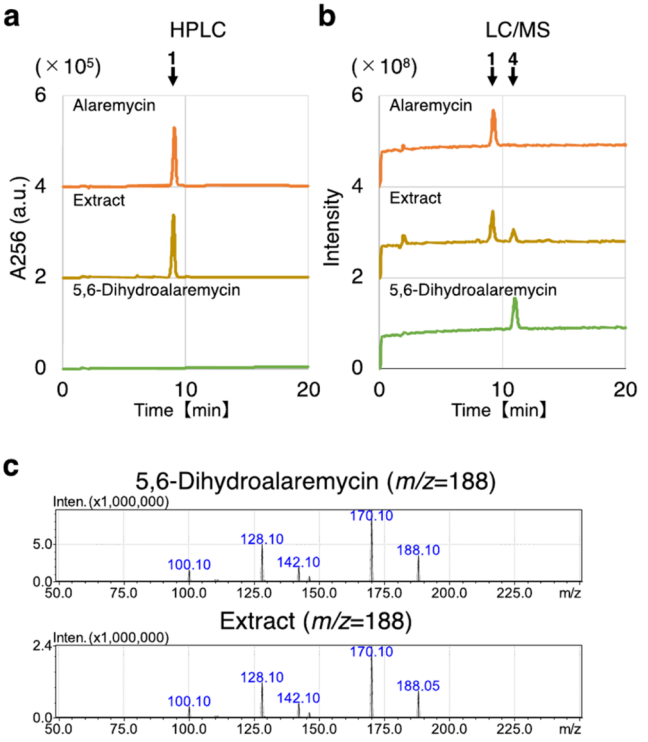

Figure 5. Identification of a new alaremycin derivative in the culture supernatant of the alaremycin-producing strain. (a) HPLC analysis of the culture supernatant from the alaremycin-producing strain A012304. Chromatograms monitored at A_{256} are shown. From top to bottom: authentic alaremycin (1), extract from the culture supernatant of A012304, and authentic 5,6-dihydroalaremycin (4). (b) LC-MS analysis of the same samples as in panel (a). Total ion chromatograms are shown. (c) MS/MS fragment patterns of the ion species with m/z = 188, derived from authentic 5,6-dihydroalaremycin (4) and the extract shown in Supporting Figure S8. Peaks corresponding to compounds 1 and 4 are indicated by arrows at the top of the chromatograms.

specifically 5,6-dihydroalaremycin (5-acetamido-4-oxohexanoic acid, **4**). We had previously synthesized **4** during a structure−activity relationship study of **1**.[19] As shown in Figure 5a,b, authentic **4** eluted at the same retention time as the unknown substance in the LC-MS analysis, which was undetectable in HPLC at A_{256}. Additionally, the MS/MS spectra of the two compounds were a perfect match (Figure 5c). Based on this evidence, we concluded that the A012304 strain produces both **1** and **4**. Judging by their ion intensities in the LC-MS analysis, the production level of **4** appeared to be lower than that of **1**.

Determination of the Biosynthetic Pathway of 5,6-Dihydroalaremycin

We next investigated the biosynthetic pathway of **4**. Considering the structural differences between **1** and **4**, we hypothesized two possible biosynthetic routes for **4** (Supporting Figure S9). One possibility is that **4** is formed by hydrogenation of the C5−C6 bond in **1** via an unknown enzyme. The other possibility is that compound **4** is synthesized by AlmA and AlmB using L-alanine as the amino acid precursor instead of L-serine, proceeding through 5-amino-4-oxohexanoic acid (**5**). In the first scenario, all three enzymes (AlmA, AlmB, and AlmC) are required to produce **4**, whereas in the second scenario, AlmC is not necessary.

As shown in Figure 6a and Supporting Figure S10, *E. coli* transformed with the palmABCE construct produced **4**, though

https://doi.org/10.1021/acsbiomedchemau.5c00045
ACS Bio Med Chem Au 2025, 5, 310−319

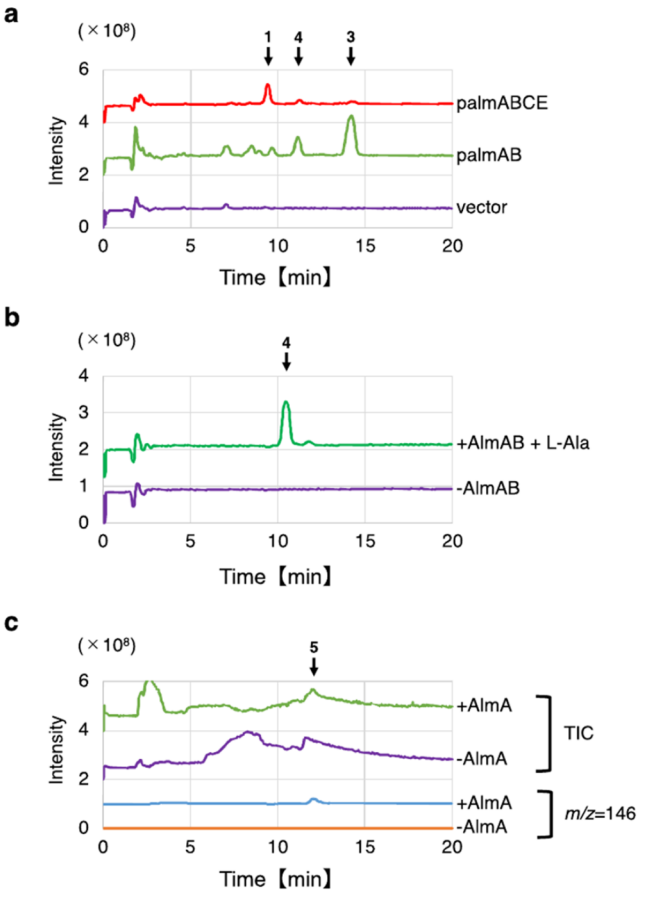

Figure 6. Biosynthesis of 5,6-dihydroalaremycin (4) *in vivo* and *in vitro*. Total ion chromatograms (TICs) of ethyl acetate extract fractions are shown. Ion peaks derived from 1, 3, 4, and 5 are indicated by arrows on the top of the chromatograms. (a) LC-MS analysis of the culture supernatants of *E. coli* cells transformed with plasmids carrying alaremycin biosynthetic genes. Top, *E. coli* transformed with palmABCE; middle, palmAB; bottom, vector control. (b) LC-MS analysis of the *in vitro* reaction mixtures. Enzymatic reactions were performed with 200 mM L-alanine, 1 mM succinyl-CoA, 20 μM PLP, and 1 mM acetyl-CoA in the presence (+AlmAB+L-Ala) or absence (−AlmAB) of 2 μM AlmA and 2 μM AlmB. (c) Enzymatic reactions were performed with 200 mM L-alanine, 1 mM succinyl-CoA, and 20 μM PLP in the presence (+AlmA) or absence (−AlmA) of 2 μM AlmA. The extracted ion chromatograms (m/z = 146) are shown below the TIC.

in smaller amounts than **1**, indicating that the alaremycin biosynthetic gene cluster is involved in the formation of **4**. Additionally, *E. coli* transformed with the palmAB construct also produced **4**, albeit in smaller amounts than **3**. This clearly indicates that AlmA and AlmB synthesize **4** in the absence of AlmC. This finding was further confirmed by *in vitro* enzyme assays. As shown in Figure 6b, AlmA and AlmB synthesized **4** *in vitro* using L-alanine as the amino acid precursor instead of L-serine. Additionally, AlmA produced intermediate **5** using L-alanine. An ion species with m/z = 146 was detected, which corresponds to the expected m/z value of the protonated form of compound **5** (M_W = 145) (Figure 6c and Supporting Figure S11).

Selectivity of L- or D-Form Amino Acids as Substrates by AlmA

As demonstrated in the *in vitro* enzyme reactions, **3** and **4** were synthesized from the L-form (*S*-form) amino acids, L-serine and L-alanine, respectively. *In vivo*, D-serine is virtually absent in both *Streptomyces* and *E. coli* cells, as they lack genes encoding serine racemase. However, significant amounts of D-alanine are present in cells, as it is utilized in peptidoglycan synthesis. We investigated whether AlmA can accept D-form amino acids as substrates *in vitro*. As shown in Figure 7a and Supporting Figure S12, the production of **3** was observed when D-serine was used as a substrate, although in smaller quantities compared to L-serine. On the other hand, when D-alanine was used as a substrate, the production of **4** was scarcely detected (Figure 7b). Based on these results, it is suggested that *Streptomyces* sp. A012304 and *E. coli* transformed with the biosynthetic genes primarily produce **3** and **4** using L-serine and L-alanine, respectively, as substrates.

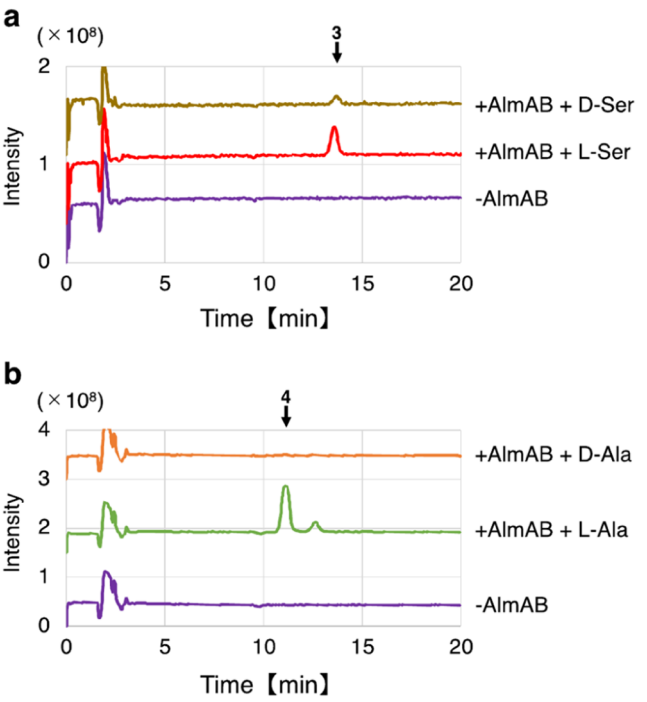

Figure 7. Selectivity of L- and D-amino acids by AlmA. LC-MS analysis of *in vitro* enzyme reaction mixtures. Total ion chromatograms of ethyl acetate extract fractions are shown. Ion peaks corresponding to compounds 3 and 4 are indicated by arrows at the top of the chromatograms. Enzymatic reactions were performed with 200 mM amino acid, 1 mM succinyl-CoA, 20 μM PLP, and 1 mM acetyl-CoA in the presence or absence of 2 μM AlmA and 2 μM AlmB. (a) From top to bottom: D-serine with AlmAB, L-serine with AlmAB, and D-serine without AlmAB. (b) From top to bottom: D-alanine with AlmAB, L-alanine with AlmAB, and without AlmAB.

Compounds **2**−**5** contain a chiral center at position C5, derived from the α-carbon of their amino acid substrates, L-serine or L-alanine. Based on the reaction mechanism of ALAS,[25] during the AlmA-catalyzed reaction, the amino acid substrate is transiently bound to the cofactor PLP. At this stage, a double bond is formed between the α-carbon of the amino acid and the amino group. Consequently, the stereochemistry at the C5 position appears to be independent of the stereochemistry of the amino acid substrate.

The stereochemistry of compound **4** was determined by using chiral column chromatography. Unexpectedly, we found that the authentic compound **4** used in this study existed as a racemic mixture. In contrast, compound **4** synthesized by

https://doi.org/10.1021/acsbiomedchemau.5c00045
ACS Bio Med Chem Au 2025, 5, 310−319

AlmA and AlmB using L-alanine as the substrate was a single enantiomer, which was coeluted with the later-eluting enantiomer of the authentic compound **4** (Supporting Figure 13S). Since the chiral column employed tends to retain *S*-form enantiomers more strongly than *R*-form enantiomers (https://www.scas.co.jp/en/technical-informations/technical-news/pdf/tn259E.pdf), it is likely that the biologically synthesized compound **4** is the *S*-form enantiomer. However, further confirmation is required in future studies.

Recently, serine palmitoyltransferase (SPT), a member of the α-oxoamine synthase family that catalyzes the condensation of L-serine and palmitoyl-CoA, has been reported to exhibit serine racemase activity.[26] Given that AlmA can accept both L- and D-serine as substrates, it is possible that AlmA also possesses racemase activity. This hypothesis should be experimentally validated for AlmA.

DISCUSSION

In this study, we elucidated the biosynthetic pathway of alaremycin (**1**) and its novel derivative, 5,6-dihydroalaremycin (**4**). Their chemical structures resemble that of 5-amino-levulinic acid (ALA), a precursor of porphyrins and a type of nonproteinogenic amino acid. This is the first report detailing the biosynthetic pathway of antibiotics containing α-oxoamine structure.

In our previous paper, we identified the biosynthetic gene cluster of **1**, which consists of the *almA*, *almB*, *almC*, and *almE* genes (Figure 1a), and proposed a possible biosynthetic pathway for **1** (Figure 1b).[20] To verify the proposed pathway, we identified intermediate molecules using the LC-MS/MS analysis with extracts from *E. coli* cells transformed with the biosynthetic genes and performed *in vitro* reconstitution of enzyme reactions using purified enzymes. As a result, we confirmed that the proposed pathway is fundamentally correct. The biosynthesis of **1** begins with the AlmA-catalyzed reaction, which condenses L-serine and succinyl-CoA, using PLP as a cofactor, to produce the first intermediate **2**. Then, AlmB catalyzes the acetylation of the amino group of **2**, using acetyl-CoA as an acetyl group donor, to produce the second intermediate **3**. Finally, AlmC catalyzes the dehydration of **3** at the C5−C6 position, using NADH and Fe^{3+} as cofactors, to yield the final product **1**.

Additionally, we discovered a novel derivative of **1** in the culture supernatant of alaremycin-producing strain A012304. Its chemical structure was identified as 5-acetamido-4-oxohexanoic acid (**4**). We also elucidated its biosynthetic pathway through the LC-MS/MS analysis and *in vitro* enzymatic reactions. **4** is synthesized using L-alanine as the amino acid precursor, instead of L-serine, by AlmA and AlmB, without the involvement of AlmC.

The structures of compounds **2**, **3**, and **5** were determined solely through the LC-MS/MS analysis. These should be confirmed in future studies using the NMR analysis or by comparison with synthetic standards.

This study revealed that AlmA can accept L-alanine as an amino acid substrate. Furthermore, *in vitro* enzyme reactions showed that AlmA also accepts D-serine. These findings expand our understanding that AlmA has a more promiscuous substrate specificity than previously thought.[20] Given that ancestral enzymes are often associated with promiscuous substrate specificity,[27,28] the ancestral form of AlmA may have had a much broader substrate range, potentially leading to the production of various ALA analogs. This characteristic of substrate specificity could be valuable in the discovery of novel bioactive molecules that affect ALA-related metabolism including porphyrin biosynthesis. Meanwhile, SPT, which catalyzes the PLP-dependent condensation of L-serine and palmitoyl-CoA, is known for its promiscuous specificity toward acyl-CoA substrates.[29] It is, therefore, possible that the acyl-CoA substrate for AlmA is not limited to succinyl-CoA alone. To further explore novel bioactive compounds and better understand AlmA's physiological role, its substrate specificity requires additional investigation.

The AlmB protein is annotated as an *N*-acetyltransferase, and it was demonstrated here that AlmB catalyzes the acetylation of the amino group of **2**, which is derived from L-serine. AlmB also accepts **5**, which is derived from L-alanine, as a substrate. This suggests that AlmB, like AlmA, exhibits a broad substrate selectivity. We are particularly interested in whether AlmB can accept ALA, which is derived from glycine, as a substrate. If so, the AlmB reaction could compete with porphyrin biosynthesis by consuming intracellular ALA. This will be investigated in a future study.

AlmC is annotated as an oxidoreductase belonging to the Gfo/Idh/MocA family. Enzymes in this family catalyze a variety of chemical reactions, including the oxidation and reduction of carbohydrates, the oxidation of trans-dihydrodiols, the reduction of biliverdin, and the hydrolysis of glycosidic bonds.[23] Interestingly, this study revealed that AlmC catalyzes the dehydration of **3** to produce **1**, using NADH and Fe^{3+} as cofactors. It is unusual for enzymes in this family to catalyze a dehydration reaction rather than dehydrogenation.[23] In the *in vitro* enzymatic reaction, AlmC consumed **3** as a substrate when only NADH was added, but no intermediate molecules were detected. The simultaneous addition of Fe^{3+} alongside NADH was required to complete the AlmC reaction and produce **1**. This suggests that reduction by NADH and oxidation by Fe^{3+} occur sequentially. Identification of the intermediate molecule formed in the presence of NADH alone is necessary to further understand the mechanism behind this unique dehydration reaction catalyzed by AlmC.

Naturally isolated antibiotics are often chemically modified to enhance their antibiotic activity and fine-tune their biophysical properties. Many clinical drugs have been developed through semisynthesis.[30−32] Recently, synthetic biology approaches have been employed to produce new antibiotic derivatives. In particular, bioengineering of polyketide synthases (PKSs) and nonribosomal peptide synthetases (NRPSs) has been extensively explored to modify polyketide-type and nonribosomal peptide antibiotics. Replacing or shuffling the modular units of PKSs or NRPSs can lead to the biosynthesis of new derivatives with novel backbones.[33−37] Targeted mutagenesis of the substrate-binding domain is also a promising strategy for generating new derivatives.[38,39] In this study, we demonstrated that two derivatives were synthesized from different starting materials: **1** from L-serine and **4** from L-alanine. Our previous study showed that amino acid substitutions around the substrate-binding pocket of AlmA altered its substrate selectivity. Specifically, substitutions at the 82nd and 86th amino acid residues of AlmA changed its affinity for L-serine and glycine.[20] Further substitutions in AlmA may enable the activation of alternative substrates.

Moreover, AlmA homologues are widely distributed across the bacterial domain, not only within the Actinobacteria phylum, to which the alaremycin-producing strain A012304 belongs, but also in other phyla, including Firmicutes and

https://doi.org/10.1021/acsbiomedchemau.5c00045
ACS Bio Med Chem Au 2025, 5, 310−319

Proteobacteria.[20] Among the α-oxoamine synthase family, to which AlmA belongs, there are enzymes that utilize amino acids and acyl-CoA substrates other than L-serine and succinyl-CoA. Examples include 8-amino-7-oxononanoate synthase (which uses L-alanine and pimeloyl-CoA),[40−42] glycine *C*-acetyltransferase (which uses glycine and acetyl-CoA),[43] and SPT (which uses L-serine and palmitoyl-CoA).[29,44] Screening for AlmA homologues with different substrate selectivities presents an attractive strategy for discovering new derivatives of alaremycin.

METHODS

Bacterial Strains and Growth Media

The alaremycin-producing strain *Streptomyces* sp. A012304 was cultured in C4 broth (2.0% glucose, 1.0% starch [potato], 0.1% Ehrlich extract, 0.4% yeast extract, 2.5% soybean meal, 0.2% NaCl, 0.1% KH_2PO_4, pH 7) at 30 °C for 6 days. *E. coli* JM109 was grown in M9 minimal medium (6.8 g/L Na_2HPO_4, 3.0 g/L KH_2PO_4, 0.5 g/L NaCl, 1.0 g/L NH_4Cl, 2 mM $MgSO_4$, 0.1 mM $CaCl_2$, 1% or 5% glucose, 10 μM $FeSO_4$) at 30 °C for 8 h to produce alaremycin and its derivatives. *E. coli* BL21(DE3) was cultured in L broth (1% polypeptone, 0.5% yeast extract, 0.5% NaCl, 0.1% glucose, pH 7) for the purification of His-tagged proteins. Ampicillin (50 μg/mL) or kanamycin (20 μg/mL) was added for the selection of *E. coli* strains carrying plasmids, and IPTG (0.5 or 1 mM) was used to induce the expression of alaremycin biosynthetic genes or genes encoding His-tagged proteins.

Construction of Plasmids

The construction of plasmids carrying the alaremycin biosynthetic genes (palmA, palmAB, palmABC, and palmABCE), as well as the plasmid for AlmA purification (pET-almA), has been previously described.[20] Plasmids for the purification of AlmB or AlmC were constructed similarly to pET-almA. Briefly, DNA fragments containing the *almB* or *almC* gene were PCR-amplified using genomic DNA from the A012304 strain as the template and a set of primers (Supporting Table S1). The amplified DNA fragments were then cloned into the pET28b(+) plasmid after digestion with the appropriate restriction enzymes. The proper construction of these plasmids was confirmed by sequencing. Primers used for PCR amplification are listed in Supporting Table S1.

Chemicals

Compound **1** was synthesized following the method of Wang et al.,[45] starting from 5-hexanoic acid and proceeding through 8 steps. ^{1}H NMR (C_2D_6OS): 2.03 (s, 3H), 2.48 (t, J = 6.3 Hz, 2H), 2.97 (t, J = 6.3 Hz, 2H), 5.80 (s, 1H), 6.47 (s, 1H), 9.12 (br s, 1H), 12.16 (br s, 1H). ^{13}C NMR (CD_3OD): δ 23.94, 29.08, 32.29, 110.71, 140.34, 172.29, 176.60, 196.94. The signals for the two olefinic protons at the terminal position (C6) were observed as singlets at 5.80 and 6.47 ppm, despite their large coupling constant.

Compound **4** was synthesized according to the method of Iwai et al.,[19] using L-alanine methyl ester hydrochloride as the starting material over 6 steps. ^{1}H NMR (C_2D_6OS): δ 1.38 (d, J = 7.0 Hz, 3H), 2.02 (s, 3H), 2.67 (t, J = 7.0 Hz, 2H), 2.86 (t, J = 7.0 Hz, 2H), 4.65 (m, J = 7.0, 1H), 6.26 (s, 1H). ^{13}C NMR (CD_3OD): δ 17.1, 23.4, 28.7, 34.2, 54.7, 170.4, 174.8, 210.0.

Authentic compounds **1** and **4** were dissolved in acetonitrile or methanol for HPLC and LC-MS/MS analyses.

HPLC and LC-MS Analyses

Culture supernatants from the alaremycin-producing strain A012304, *E. coli* strains transformed with plasmids carrying the alaremycin biosynthetic genes, or enzyme reaction mixtures were extracted three times with an equal volume of ethyl acetate at pH 2. The organic layers were collected, and the ethyl acetate was evaporated. The residues were dissolved in acetonitrile and subjected to HPLC and LC-MS analyses.

For the detection of compound **2**, culture supernatants or enzyme reaction mixtures were precipitated with four volumes of acetone at −30 °C overnight. The mixtures were centrifuged at 12,000 rpm for 2 min, and the supernatants were collected. After removal of acetone by evaporation, the supernatants were freeze-dried. The resulting residues were dissolved in acetonitrile and analyzed by using HPLC and LC-MS.

HPLC analysis was performed using a Nexera MP system (Shimadzu) equipped with a COSMOSIL HILIC column (2.0 mm ID × 150 mm, Nacalai Tesque). Metabolites were separated using an acetonitrile/30 mM ammonium acetate (80:20, v/v) solution at a flow rate of 0.2 mL/min, with the absorption monitored at 256 nm (A_{256}).

LC-MS analysis was conducted by using the HPLC system coupled to a triple quadrupole mass spectrometer (LCMS-8050, Shimadzu) in positive mode. For MS/MS analysis, selected ion monitoring was employed in positive mode with a collision energy of −5 or −10 V and full mass scans.

Chiral column chromatography was performed using the HPLC system (Prominence, Shimadzu) equipped with a SUMICHIRAL OA-4700 column (4.0 mm ID × 150 mm, Sumitomo Chemical). Compounds were separated with a solvent mixture of hexane/tetrahydrofuran/ethanol (70:20:10, v/v) supplemented with 0.2% formic acid at a flow rate of 1 mL/min, with the absorption monitored at 282 nm (A_{282}).

Protein Purification

The *E. coli* BL21(DE3) strain transformed with pET-almA, pET-almB, or pET-almC was cultured in L broth at 30 °C for 2 h. Then, 0.5 mM IPTG was added, and the culture was continued for an additional 22 h at 20 °C. The cells were harvested by centrifugation and lysed by sonication in a buffer containing 300 mM KCl, 50 mM KH_2PO_4, and 5 mM imidazole. The lysates were centrifuged at 15,300*g* for 20 min to remove insoluble materials. His-tagged proteins were purified using a Ni-resin column on a Profinia system (Bio-Rad) and eluted with a buffer containing 300 mM KCl, 50 mM KH_2PO_4, and 250 mM imidazole. The eluted fractions were desalted using 20 or 100 mM HEPES-NaOH (pH 7.5) with 6% glycerol. Protein concentrations were determined using the Advanced Protein Assay Kit (Cytoskeleton). For the AlmA protein, 20 or 100 mM HEPES-NaOH (pH 7.5), 10% glycerol, and 20 μM pyridoxal 5′-phosphate (PLP) were used for storage. The purified proteins were stored at −30 °C. Protein purity was confirmed by sodium dodecyl sulfate-polyacrylamide gel electrophoresis (SDS-PAGE).

Enzymatic Assay

Enzymatic reactions were generally performed as described below. The reaction mixture consisted of 20 or 100 mM HEPES-NaOH (pH 7.5), 3 mM $MgCl_2$, and 2 μM His-tagged protein(s). Reactions were carried out at 37 °C for 60 min.

For the AlmA reaction, 10 or 200 mM amino acid and 0.2 or 1 mM succinyl-CoA were used as substrates and 20 μM PLP was included as a cofactor.

For the AlmB reaction, AlmA, L-serine, succinyl-CoA, and PLP were added to supply a substrate for AlmB, and 0.2 or 1 mM acetyl-CoA was used as the acetyl group donor.

For the AlmC reaction, the reaction was first performed with 10 mM L-serine, 0.2 mM succinyl-CoA, 20 μM PLP, 0.2 mM acetyl-CoA, 2 μM AlmA, and 2 μM AlmB for 2 h at 30 °C to accumulate the substrate for AlmC. Then, 2 μM AlmC, 0.2 mM NADH or NAD^+, and 3 mM $FeCl_3$ were added, and the reaction mixture was further incubated for another hour. The consumption of NADH was monitored by measuring its specific absorption at 340 nm (A_{340}).

Amino acids used included L- or D-serine and L- or D-alanine. His-tagged proteins were omitted for negative controls.

https://doi.org/10.1021/acsbiomedchemau.5c00045
ACS Bio Med Chem Au 2025, 5, 310−319

ASSOCIATED CONTENT

Supporting Information

The Supporting Information is available free of charge at https://pubs.acs.org/doi/10.1021/acsbiomedchemau.5c00045.

Primer list, LC-MS chromatograms, SDS-PAGE photograph, and predicted biosynthetic pathways (PDF)

AUTHOR INFORMATION

Corresponding Author

Masaaki Wachi − *Department of Life Science and Technology, Institute of Science Tokyo, Yokohama 226-8501, Japan;* orcid.org/0000-0002-3655-4035; Email: mwachi@bio.titech.ac.jp

Authors

Mio Okui − *Department of Life Science and Technology, Institute of Science Tokyo, Yokohama 226-8501, Japan;* orcid.org/0009-0007-7914-8073

Yuki Noto − *Department of Life Science and Technology, Institute of Science Tokyo, Yokohama 226-8501, Japan;* orcid.org/0009-0007-8365-9466

Jun Kawaguchi − *Department of Life Science and Technology, Institute of Science Tokyo, Yokohama 226-8501, Japan;* Present Address: Institute of Life and Environmental Sciences, University of Tsukuba, 1−1−1 Tennodai, Tsukuba, Ibaraki 305−8577, Japan; orcid.org/0009-0007-1690-5946

Noritaka Iwai − *Department of Life Science and Technology, Institute of Science Tokyo, Yokohama 226-8501, Japan;* orcid.org/0000-0001-8014-6007

Complete contact information is available at: https://pubs.acs.org/10.1021/acsbiomedchemau.5c00045

Author Contributions

‡M.O. and Y.N. contributed equally to this work. CRediT: M.O.: data curation, formal analysis, investigation, validation, visualization, and writing—original draft; Y.N.: data curation, formal analysis, investigation, validation, visualization, and writing—review and editing; J.K.: investigation, writing—review and editing; N.I.: supervision, writing—review and editing; M.W.: conceptualization, funding acquisition, methodology, project administration, supervision, and writing—review and editing. CRediT: **Mio Okui** data curation, formal analysis, investigation, validation, visualization, writing - original draft; **Yuki Noto** data curation, formal analysis, investigation, validation, visualization, writing - review & editing; **Jun Kawaguchi** investigation, writing - review & editing; **Noritaka Iwai** supervision, writing - review & editing; **Masaaki Wachi** conceptualization, funding acquisition, methodology, project administration, supervision, writing - review & editing.

Funding

This work was partly supported by the Support for Pioneering Research Initiated by the Next Generation from the Japan Science and Technology Agency (JPMJSP2106) and JSPS Grant-in-Aid for Challenging Research (Exploratory) (JP22K19129).

Notes

The authors declare no competing financial interest.

ACKNOWLEDGMENTS

The authors thank the Center for Integrative Biosciences and the Biomaterials Analysis Division, Open Facility Center at the Tokyo Institute of Technology, for DNA sequencing and the Open Research Facilities for Life Science and Technology at the Tokyo Institute of Technology for LC-MS/MS analysis.

REFERENCES

(1) Fleming, A. On the antibacterial action of cultures of a penicillium, with special reference to their use in the isolation of *B. influenzæ*. *Br. J. Exp. Pathol.* **1929**, *10*, 226−236.

(2) Katz, L.; Baltz, R. H. Natural product discovery: past, present, and future. *J. Ind. Microbiol. Biotechnol.* **2016**, *43*, 155−176.

(3) Hutchings, M. I.; Truman, A. W.; Wilkinson, B. Antibiotics: past, present and future. *Curr. Opin. Microbiol.* **2019**, *51*, 72−80.

(4) Hirsch, E. B.; Tam, V. H. Impact of multidrug-resistant *Pseudomonas aeruginosa* infection on patient outcomes. *Expert Rev. Pharmacoeconomics Outcomes Res.* **2010**, *10*, 441−451.

(5) Coyne, A. J. K.; El Ghali, A.; Holger, D.; Rebold, N.; Rybak, M. J. Therapeutic strategies for emerging multidrug-resistant *Pseudomonas aeruginosa*. *Infect. Dis. Ther.* **2022**, *11*, 661−682.

(6) Reynolds, D.; Kollef, M. The epidemiology and pathogenesis and treatment of *Pseudomonas aeruginosa* infections: An Update. *Drugs* **2021**, *81*, 2117−2131.

(7) Belete, M. A.; Gedefie, A.; Alemayehu, E.; Debash, H.; Mohammed, O.; Gebretsadik, D.; Ebrahim, H.; Tilahun, M. The prevalence of vancomycin-resistant *Staphylococcus aureus* in Ethiopia: a systematic review and meta-analysis. *Antimicrob. Resist. Infect. Control* **2023**, *12*, No. 86.

(8) Cong, Y.; Yang, S.; Rao, X. Vancomycin resistant *Staphylococcus aureus* infections: A review of case updating and clinical features. *J. Adv. Res.* **2020**, *21*, 169−176.

(9) Li, G.; Walker, M. J.; De Oliveira, D. M. P. Vancomycin resistance in *Enterococcus* and *Staphylococcus aureus*. *Microorganisms* **2023**, *11*, No. 24.

(10) Ahmed, M. O.; Baptiste, K. E. Vancomycin-resistant Enterococci: A review of antimicrobial resistance mechanisms and perspectives of human and animal health. *Microb. Drug Resist.* **2018**, *24*, 590−606.

(11) Eichel, V. M.; Last, K.; Brühwasser, C.; von Baum, H.; Dettenkofer, M.; Götting, T.; Grundmann, H.; Güldenhöven, H.; Liese, J.; Martin, M.; Papan, C.; Sadaghiani, C.; Wendt, C.; Werner, G.; Mutters, N. T. Epidemiology and outcomes of vancomycin-resistant enterococcus infections: a systematic review and meta-analysis. *J. Hosp. Infect.* **2023**, *141*, 119−128.

(12) Khawbung, J. L.; Nath, D.; Chakraborty, S. Drug resistant tuberculosis: A review. *Comp. Immunol., Microbiol. Infect. Dis.* **2021**, *74*, No. 101574.

(13) Lange, C.; Dheda, K.; Chesov, D.; Mandalakas, A. M.; Udwadia, Z.; Horsburgh, C. R., Jr. Management of drug-resistant tuberculosis. *Lancet* **2019**, *394*, 953−966.

(14) Wulandari, D. A.; Hartati, Y. W.; Ibrahim, A. U.; Pitaloka, D. A. E.; Irkham. Multidrug-resistant tuberculosis. *Clin. Chim. Acta* **2024**, *559*, No. 119701.

(15) O'Neill, J. Drug-resistant infections globally: final report and recommendations. Review on antimicrobial resistance 2016 https://amr-review.org/sites/default/files/160525_Final%20paper_with%20cover.pdf. (accessed February 27, 2025).

(16) Wachi, M.; Iwai, N.; Kunihisa, A.; Nagai, K. Irregular nuclear localization and anucleate cell production in *Escherichia coli* induced by a Ca^{2+} chelator, EGTA. *Biochimie* **1999**, *81*, 909−913.

(17) Awa, Y.; Iwai, N.; Ueda, T.; Suzuki, K.; Asano, S.; Yamagishi, J.; Nagai, K.; Wachi, M. Isolation of a new antibiotic, alaremycin, structurally related to 5-aminolevulinic acid from *Streptomyces* sp. A012304. *Biosci. Biotechnol. Biochem.* **2005**, *69*, 1721−1725.

(18) Heinemann, I. U.; Schulz, C.; Schubert, W. D.; Heinz, D. W.; Wang, Y. G.; Kobayash, Y.; Awa, Y.; Wachi, M.; Jahn, D.; Jahn, M. Structure of the heme biosynthetic *Pseudomonas aeruginosa*

porphobilinogen synthase in complex with the antibiotic alaremycin. *Antimicrob. Agents Chemother.* **2010**, *54*, 267−272.
(19) Iwai, N.; Nakayama, K.; Oku, J.; Kitazume, T. Synthesis and antibacterial activity of alaremycin derivatives for the porphobilinogen synthase. *Bioorg. Med. Chem. Lett.* **2011**, *21*, 2812−2815.
(20) Kawaguchi, J.; Mori, H.; Iwai, N.; Wachi, M. A secondary metabolic enzyme functioned as an evolutionary seed of a primary metabolic enzyme. *Mol. Biol. Evol.* **2022**, *39*, No. msac164.
(21) Sheldon, P. J.; Mao, Y.; He, M.; Sherman, D. H. Mitomycin resistance in *Streptomyces lavendulae* includes a novel drug-binding-protein-dependent export system. *J. Bacteriol.* **1999**, *181*, 2507−2512.
(22) Yu, L.; Yan, X.; Wang, L.; Chu, J.; Zhuang, Y.; Zhang, S.; Guo, M. Molecular cloning and functional characterization of an ATP-binding cassette transporter OtrC from *Streptomyces rimosus*. *BMC Biotechnol.* **2012**, *12*, No. 52.
(23) Taberman, H.; Parkkinen, T.; Rouvinen, J. Structural and functional features of the NAD(P) dependent Gfo/Idh/MocA protein family oxidoreductases. *Protein Sci.* **2016**, *25*, 778−786.
(24) Hanukoglu, I.; Gutfinger, T. cDNA sequence of adrenodoxin reductase. Identification of NADP-binding sites in oxidoreductases. *Eur. J. Biochem.* **1989**, *180* (2), 479−484.
(25) Stojanovski, B. M.; Hunter, G. A.; Na, I.; Uversky, V. N.; Jiang, R. H. Y.; Ferreira, G. C. 5-Aminolevulinate synthase catalysis: The catcher in heme biosynthesis. *Mol. Genet. Metab.* **2019**, *128*, 178−189.
(26) Ikushiro, H.; Honda, T.; Murai, Y.; Murakami, T.; Takahashi, A.; Sawai, T.; Goto, H.; Ikushiro, S. I.; Miyahara, I.; Hirabayashi, Y.; Kamiya, N.; Monde, K.; Yano, T. Racemization of the substrate and product by serine palmitoyltransferase from *Sphingobacterium multivorum* yields two enantiomers of the product from D-serine. *J. Biol. Chem.* **2024**, *300*, No. 105728.
(27) Modi, T.; Risso, V. A.; Martinez-Rodriguez, S.; Gavira, J. A.; Mebrat, M. D.; Van Horn, W. D.; Sanchez-Ruiz, J. M.; Ozkan, S. B. Hinge-shift mechanism as a protein design principle for the evolution of β-lactamases from substrate promiscuity to specificity. *Nat. Commun.* **2021**, *12*, No. 1852.
(28) Zou, T.; Risso, V. A.; Gavira, J. A.; Sanchez-Ruiz, J. M.; Ozkan, S. B. Evolution of conformational dynamics determines the conversion of a promiscuous generalist into a specialist enzyme. *Mol. Biol. Evol.* **2015**, *32*, 132−143.
(29) Hanada, K. Serine palmitoyltransferase, a key enzyme of sphingolipid metabolism. *Biochim. Biophys. Acta, Mol. Cell Biol. Lipids* **2003**, *1632*, 16−30.
(30) Butler, M. S. The role of natural product chemistry in drug discovery. *J. Nat. Prod.* **2004**, *67*, 2141−2153.
(31) Goel, B.; Tripathi, N.; Bhardwaj, N.; Singh, I. P.; Jain, S. K. Semisynthesis: An essential tool for antibiotics drug discovery. *ChemistrySelect* **2024**, *9*, No. e202400554.
(32) Wright, P. M.; Seiple, I. B.; Myers, A. G. The evolving role of chemical synthesis in antibacterial drug discovery. *Angew. Chem., Int. Ed.* **2014**, *53*, 8840−8869.
(33) Bozhüyük, K. A.; Micklefield, J.; Wilkinson, B. Engineering enzymatic assembly lines to produce new antibiotics. *Curr. Opin. Microbiol.* **2019**, *51*, 88−96.
(34) Camus, A.; Gantz, M.; Hilvert, D. High-throughput engineering of nonribosomal extension modules. *ACS Chem. Biol.* **2023**, *18*, 2516−2523.
(35) Cummings, M.; Breitling, R.; Takano, E. Steps towards the synthetic biology of polyketide biosynthesis. *FEMS Microbiol. Lett.* **2014**, *351*, 116−125.
(36) Klaus, M.; Grininger, M. Engineering strategies for rational polyketide synthase design. *Nat. Prod. Rep.* **2018**, *35*, 1070−1081.
(37) Nava, A. A.; Roberts, J.; Haushalter, R. W.; Wang, Z.; Keasling, J. D. Module-based polyketide synthase engineering for *de novo* polyketide biosynthesis. *ACS Synth. Biol.* **2023**, *12*, 3148−3155.
(38) Bravo-Rodriguez, K.; Klopries, S.; Koopmans, K. R. M.; Sundermann, U.; Yahiaoui, S.; Arens, J.; Kushnir, S.; Schulz, F.; Sanchez-Garcia, E. Substrate flexibility of a mutated acyltransferase domain and implications for polyketide biosynthesis. *Chem. Biol.* **2015**, *22*, 1425−1430.
(39) Sundermann, U.; Bravo-Rodriguez, K.; Klopries, S.; Kushnir, S.; Gomez, H.; Sanchez-Garcia, E.; Schulz, F. Enzyme-directed mutasynthesis: a combined experimental and theoretical approach to substrate recognition of a polyketide synthase. *ACS Chem. Biol.* **2013**, *8*, 443−450.
(40) Alexander, F. W.; Sandmeier, E.; Mehta, P. K.; Christen, P. Evolutionary relationships among pyridoxal-5′-phosphate-dependent enzymes. Regio-specific alpha, beta and gamma families. *Eur. J. Biochem.* **1994**, *219*, 953−960.
(41) Mann, S.; Ploux, O. Pyridoxal-5′-phosphate-dependent enzymes involved in biotin biosynthesis: structure, reaction mechanism and inhibition. *Biochim. Biophys. Acta, Proteins Proteomics* **2011**, *1814*, 1459−1466.
(42) Manandhar, M.; Cronan, J. E. A Canonical biotin synthesis enzyme, 8-amino-7-oxononanoate synthase (BioF), utilizes different acyl chain donors in *Bacillus subtilis* and *Escherichia coli*. *Appl. Environ. Microbiol.* **2018**, *84*, No. e02084-17.
(43) Marcus, J. P.; Dekker, E. E. Threonine formation via the coupled activity of 2-amino-3-ketobutyrate coenzyme A lyase and threonine dehydrogenase. *J. Bacteriol.* **1993**, *175*, 6505−6511.
(44) Lowther, J.; Charmier, G.; Raman, M. C.; Ikushiro, H.; Hayashi, H.; Campopiano, D. J. Role of a conserved arginine residue during catalysis in serine palmitoyltransferase. *FEBS Lett.* **2011**, *585*, 1729−1734.
(45) Wang, Y.; Wachi, M.; Kobayashi, Y. Synthesis of alaremycin. *Synlett* **2006**, *0*, 0481−0483.

https://doi.org/10.1021/acsbiomedchemau.5c00045
ACS Bio Med Chem Au 2025, 5, 310−319